Asociación Argentina
de Mecánica Computacional

Mecánica Computacional Vol XXVIII, págs. 343-362 (artículo completo)
Cristian García Bauza, Pablo Lotito, Lisandro Parente, Marcelo Vénere (Eds.)
Tandil, Argentina, 3-6 Noviembre 2009

THE EFFECT OF CONFINEMENT AND STAND-OFF DISTANCE IN BLAST TESTS

Daniel Ambrosini[a,c], Bibiana Luccioni[b,c], Gerald Nurick[d], Genevieve Langdon[d] and Neville Jacob[d]

[a]*Maestría en Ingeniería Estructural, Facultad de Ingeniería, Universidad Nacional de Cuyo Centro Universitario - Parque Gral. San Martín - 5500 Mendoza, dambrosini@uncu.edu.ar*
http://fing.uncu.edu.ar/academico/posgrados/estructural/maestria-en-ingenieria-estructural

[b]*Instituto de Estructuras, Universidad Nacional de Tucumán, Av. Roca 1800, 4000 S.M. de Tucumán , Argentina, blucciont@herrera.unt.edu.ar.edu.ar , www.herrera.unt.edu.ar/iest*

[c]*CONICET*

[d]*Blast Impact and Survivability Research Unit (BISRU), Department of Mechanical Engineering, University of Cape Town, Rondebosch 7701, South Africa. Gerald.Nurick@uct.ac.za*
http://www.bisru.uct.ac.za

Keywords: Explosion, blast wave, numerical model, overpressure, impulse

Abstract. In recent years the explosive loads have received considerable attention due to different events, accidental or intentional, that have occured over important structures all over the world. In consequence, in the last decade there was an important activity in the research of explosive loads. Initially, this works were mostly empirical, but, in the last years, important researches have begun to be developed.

Much of this work has concentrated on the response of monolithic metal beams and plates to impulsive loads. In particular, a set of experimental tests about clamped circular mild steel plates, of radius 53 mm, subjected to blast loads travelling along tubular structures was carried out at the Blast Impact and Survivability Research Unit (BISRU, University of Cape Town). Some counter-intuitive results about incident impulse and plate response were observed in the experiments.

The main objective of this paper is to study numerically the wave propagation in the tube used for the tests and to compare the response with that obtained experimentally. The effects of confinement, stand-off distance and charge mass on the reflected pressures and impulses are studied. The stand-off distance is varied from 25 to 300 mm, and the load masses are varied from 4 to 15 g. Finally, the effect of the reflection on the plate is also analyzed. The analysis shows satisfactory correlation with experimental results.

Copyright © 2009 Asociación Argentina de Mecánica Computacional http://www.amcaonline.org.ar

1 INTRODUCTION

Blasting loads have come to be forefront of attention in recent years due to a number of accidental and intentional events that affected important structures all over the world, clearly indicating that this issue is important for purposes of structural design and reliability analysis. In consequence, extensive research activities in the field of blast loads have taken place in the last few decades.

Generally, simplifying assumptions must be made in order to solve specific problems. Until now, most practical problems have been solved through empirical approaches. Years of industrial and military experience have been condensed in charts or equations (Baker et al. 1983, Kinney and Graham 1985). However, with the rapid development of computer hardware over the last years, it has become possible to make detailed numerical simulations of explosive events in personal computers, significantly increasing the availability of these methods. New developments in integrated computer hydrocodes complete the tools necessary to carry out the numerical analysis successfully. Nevertheless, it is important to be aware that both these models and analysis procedures still need experimental validation.

On the other hand, the response of fully clamped metal plates subjected to uniform and localized blast loads has been studied for many years. Experimental work on beams, plates and shells has been widely reported. Nurick and Martin (1989) presented an overview of theoretical and experimental results that dealt mostly with uniformly loaded plates. In subsequent years, mild steel plates subjected to localized blast loads are reported by Chung Kim Yuen S and Nurick (2000) and Jacob et al. (2004).

The failure of circular plates subjected to *uniform* blast loads was investigated by Teeling-Smith and Nurick (1991). It was reported that permanent midpoint deflection increased with increasing impulse, resulting in thinning at the boundary. Further increases in impulse led to partial tearing along the plate boundary, followed by complete tearing. The mid-point deflection decreased as impulse was increased beyond the threshold of complete tearing, as the failure tended towards complete shear at the boundary edge. Schleyer et al. (2003) examined the effect of boundary clamping on the response of mild steel plates subjected to dynamic loading. The loading took the form of a triangular pressure pulse applied over 50 ms and was not impulsive considering the long load duration with respect to the natural period of the test plates.

Experiments on fully clamped circular mild steel plates subjected to *localized* blast loads were reported by Nurick and Radford (1997). The plate deformation was characterised by an inner dome superimposed on a larger global dome, later reported by Jacob et al. (2004) for built-in circular plates and for quadrangular plates subjected to localised loads. At higher impulses, thinning at the central area and boundary of the plate was observed. Tearing in the central area of the plate occurred with further increases in impulse after the onset of thinning. The tearing observed was characterized by a cap torn away from the plate. Tearing at the boundary was observed for larger load diameter— plate diameter ratios.

Although there are numerous empirical relationships relating stand-off distance to blast overpressure for free-field explosions, the relationship between stand-off distance and plate deformation due to air blast is not widely reported. There are no established relationships for predicting either the response of plate or the characteristics of the blast loading when the explosion is partially confined.

Related to this problem a set of experimental tests about clamped circular mild steel plates, of radius 53 mm, subjected to blast loads travelling along tubular structures was carried out at the Blast Impact and Survivability Research Unit (BISRU, University of Cape Town). Some counter-intuitive results about incident impulse and plate response were observed in the

Copyright © 2009 Asociación Argentina de Mecánica Computacional http://www.amcaonline.org.ar

experiments (Jacob et al. 2007).

Then, the main objective of this paper is to study numerically the wave propagation in the tube used for the tests and to compare the response with that obtained experimentally. The effects of confinement, stand-off distance and charge mass on the reflected pressures and impulses are studied. The stand-off distance is varied from 25 to 300 mm, and the load masses are varied from 4 to 15 g.

2 DESCRIPTION OF THE TESTS AND MAIN FINDINGS

The test specimens are 244 mm by 244 mm by 1.9 mm thick. The specimens are clamped in a test rig, comprising two (244 mm × 244 mm) frames made from 20 mm thick mild steel plating. A tube of required length, selected from the range shown in Fig. 1, is screwed onto the front clamping frame and the rear clamping frame has a hole of diameter 106 mm, the same as the internal diameter of the tube as shown in Fig. 2. Therefore, each test specimen has a circular exposed area with a diameter of 106 mm. In the case of the smallest (13 mm) stand-off distance, the explosive charge is placed on a 13 mm thick polystyrene pad mounted directly onto the plate. For stand-off distances ranging from 25 to 300 mm, mild steel tubes of internal diameter 106 mm are used. This technique employs tubes to improve the spatial uniformity of the blast loading incident on the target plate. There are no empirical equations relating the influence of stand-off distance to blast loading that is constrained to propagate in this way (Jacob et al. 2007).

Figure 1: Photograph of mild steel tubes used in the experiments (Jacob et al. 2007).

The test rig is attached to a ballistic pendulum using four spacer rods. The oscillation amplitude of the pendulum is used to determine the impulse imparted to the plates, given the mass of the pendulum and the geometry in accordance with other works (Nurick and Radford 1997, Jacob et al. 2004). The rods allow the plate to deform without coming in contact with the I-beam of the pendulum. A photograph of the experimental set-up is shown in Fig. 3. Plastic explosive PE4 is moulded into a polystyrene disc with a diameter of 34 mm and sited at the open end of the tube (Fig. 4). A 1 g leader of explosive is used to attach the detonator to the main charge, thus the total mass of explosive is the sum of the disc and the 1 g leader. The

Copyright © 2009 Asociación Argentina de Mecánica Computacional http://www.amcaonline.org.ar

inclusive charge masses range from 4 to 15 g. The stand-off distance is equal to the length of the tube. The experimental details are given Jacob et al. (2007).

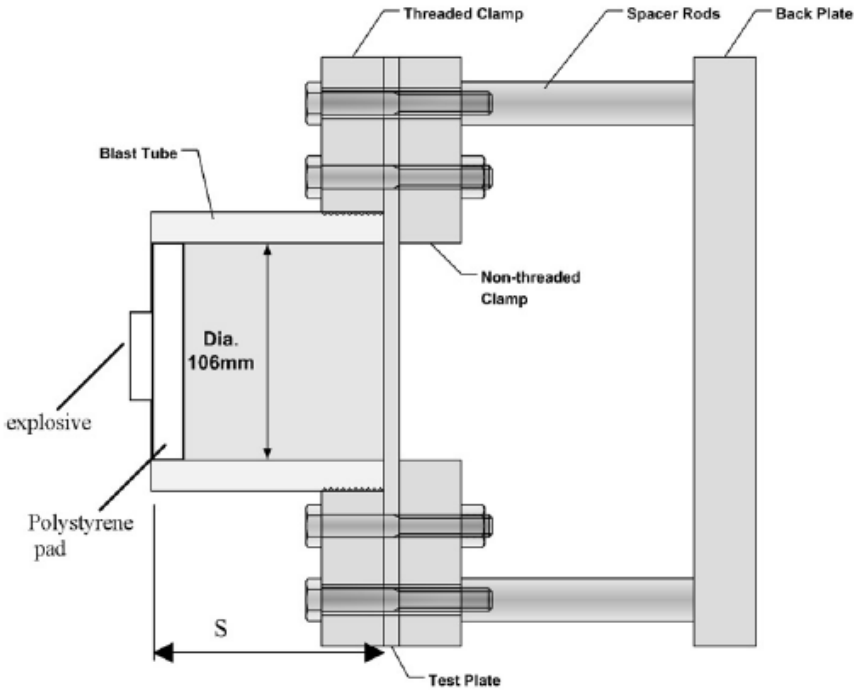

Figure 2: Schematic of the experimental test rig (Jacob et al. 2007)

Figure 3: Test rig attached to the ballistic pendulum

Copyright © 2009 Asociación Argentina de Mecánica Computacional http://www.amcaonline.org.ar

Figure 4: Polystyrene pad

2.1 Main results

It was shown by Jacob et al. (2007) that stand-off distance influences the type of loading condition applied to a structure. This is illustrated by different plate profiles observed at various stand-off distances. An inner dome superimposed on a larger global dome is seen at stand-off distances ranging from 13 to 40 mm indicating a localisation of the blast load on the plate for stand-off distance less than plate radius. In the case of stand-off distance greater than 100 mm, the plate profile is a global dome indicating uniform distribution of the blast load. At stand-off distances of 50 and 75 mm, it appears that a transition in loading condition occurs. This is represented by plate response showing aspects of uniform and localized loading. The results show that midpoint deflections decrease significantly as stand-off distance increases from 13 to 50 mm for a given charge mass. In the case of stand-off distances ranging from 75 to 300 mm, similar midpoint deflections are obtained.

3 NUMERICAL MODEL

3.1 Introduction and numerical tool

Computer codes normally referred as “hydrocodes” encompass several different numerical techniques in order to solve a wide variety of non-linear problems in solid, fluid and gas dynamics. The phenomena to be studied with such a program can be characterized as highly time dependent with both geometric non-linearities (e.g. large strains and deformations) and material non-linearities (e.g. plasticity, failure, strain-hardening and softening, multiphase equations of state).

In this paper, the software AUTODYN-3D (2007), which is a “hydrocode” that uses finite difference, finite volume, and finite element techniques to solve a wide variety of non-linear problems in solid, fluid and gas dynamics, is used. The phenomena to be studied with such a

Copyright © 2009 Asociación Argentina de Mecánica Computacional http://www.amcaonline.org.ar

program can be characterized as highly time dependent with both geometric non-linearities (e.g. large strains and deformations) and material non-linearities (e.g. plasticity, failure, strain-hardening and softening, multiphase equations of state).

The various numerical processors available in AUTODYN generally use a coupled finite difference/finite volume approach similar to that described by Cowler and Hancock (1979). This scheme allows alternative numerical processors to be selectively used to model different components/regimes of a problem. Individual structured meshes operated on by these different numerical processors can be coupled together in space and time to efficiently compute structural, fluid, or gas dynamics problems including coupled problems (e.g. fluid-structure, gas-structure, structure-structure, etc.).

AUTODYN includes the following numerical processors: Lagrange, Euler, ALE, Shell, Euler-Godunov, Euler-FCT and SPH. All the above processors use explicit time integration. The first-order Euler approach scheme is based on the method developed by Hancock (1976).

While finite element codes are usually based on the equilibrium condition, the hydrocode utilizes the differential equations governing unsteady material dynamic motion: the local conservation of mass, momentum and energy. In order to obtain a complete solution, in addition to appropriate initial and boundary conditions, it is necessary to define a further relation between the flow variables. This can be found from a material model, which relates stress to deformation and internal energy (or temperature). In most cases, the stress tensor may be separated into a uniform hydrostatic pressure (all three normal stresses equal) and a stress deviatoric tensor associated with the resistance of the material to shear distortion.

3.2 Material models

a) Air: The ideal gas equation of state was used for the air. This is one of the simplest forms of equation of state for gases. In an ideal gas, the internal energy is a function of the temperature alone and if the gas is polytropic the internal energy is simply proportional to temperature. It follows that the equation of state for a gas, which has uniform initial conditions, may be written as,

$$p = (\gamma - 1)\rho e \tag{1}$$

in which p is the hydrostatic pressure, ρ is the density and e is the specific internal energy. γ is the adiabatic exponent**,** it is a constant (equal to $1 + R/c_v$) where constant R may be taken to be the universal gas constant R_0 divided by the effective molecular weight of the particular gas and c_v is the specific heat at constant volume.

b) TNT: High explosives are chemical substances which, when subject to suitable stimuli, react chemically very rapidly (in order of microseconds) releasing energy. In the hydrodynamic theory of detonation, this very rapid time interval is shrunk to zero and a detonation wave is assumed to be a discontinuity which propagates through the unreacted material instantaneously liberating energy and transforming the explosive into detonating products. The normal Rankine-Hugoniot relations, expressing the conservation of mass, momentum and energy across the discontinuity may be used to relate the hydrodynamic variables across the reaction zone. The only difference between the Rankine-Hugoniot equations for a shock wave in a chemically inert material and those for a detonation wave is the inclusion of a chemical energy term in the energy conservation equation.

Since the 1939-45 war, when there was naturally extensive study of the behaviour of high explosives, there has been a continuous attempt to understand the detonation process and the performance of the detonation products, leading to considerable improvements in the equation of state of the products. The most comprehensive form of equation of state developed over

Copyright © 2009 Asociación Argentina de Mecánica Computacional http://www.amcaonline.org.ar

this period, the "Jones - Wilkins - Lee" (JWL) equation of state, is used in this paper.

$$p = C_1\left(1-\frac{\omega}{r_1 v}\right)e^{-r_1 v} + C_2\left(1-\frac{\omega}{r_2 v}\right)e^{-r_2 v} + \frac{\omega e}{v} \tag{2}$$

Where $v = 1/\rho$ is the specific volume, C_1, r_1, C_2, r_2 and ω (adiabatic constant) are constants and their values have been determined from dynamic experiments and are available in the literature for many common explosives.

It can be shown that at large expansion ratios the first and second terms on the right hand side of Equation (4) become negligible and hence the behaviour of the explosive tends towards that of an ideal gas. Therefore, at large expansion ratios, where the explosive has expanded by a factor of approximately 10 from its original volume, it is valid to switch the equation of state for a high explosive from JWL to ideal gas. In such a case the adiabatic exponent for the ideal gas, γ, is related to the adiabatic constant of the explosive, ω, by the relation $\gamma=\omega+1$. The reference density for the explosive can then be modified and the material compression will be reset. Potential numerical difficulties are therefore avoided.

An explosion may be initiated by various methods. However, whether an explosive is dropped, thermally irradiated or shocked, either mechanically or from a shock from an initiator (of more sensitive explosive), initiation of an explosive always goes through a stage in which a shock wave is an important feature. Lee-Tarver equation of state (Lee and Tarver 1980) was used to model both the detonation and expansion of TNT in conjunction with JWL EOS to model the unreacted explosive.

In order to obtain the TNT-equivalency between TNT and PE4, the results presented by Wharton et al. (2000) were used. Then, a 1.3 equivalency was used in this paper. In Table 1 the masses of charges analyzed and its TNT-equivalency are presented. Consider that all loads are cylinder with 34 mm of diameter and taking into account the mass density of TNT (1.63 g/cm^3) the height of the explosive cylinder is also presented in Table 1.

Mass PE4 g	Mass TNT g	TNT height mm
4	5.2	3.5
9	11.7	7.9
15	19.5	13.2

Table 1: Equivalent masses of the loads used and height of the cylinder.

c) Plate: In this first stage of the study, the clamped circular mild steel plates were considered rigid. The influence of the flexibility of the plates will be presented in subsequent papers.

3.3 Numerical meshes

In this paper, an Euler Godunov processor is used to model the air as well as the explosive charge. The use of symmetry conditions allows using a two-dimensional (2D) mesh considering axial symmetry. The number of cells required to produce accurate solutions is greatly reduced when compared with a full 3D model.

For each case of blast load listed in Table 1, the following stand-off distances were used: 25, 50, 75, 100, 200 and 300 mm. The numerical models for different cases are shown in Figures 5 and 6. In all cases, the detonation point is represented by a red point. Also, the gauge points in which all variables of interest are saved and the boundary transmit are

Copyright © 2009 Asociación Argentina de Mecánica Computacional http://www.amcaonline.org.ar

presented in Figures 5 and 6.

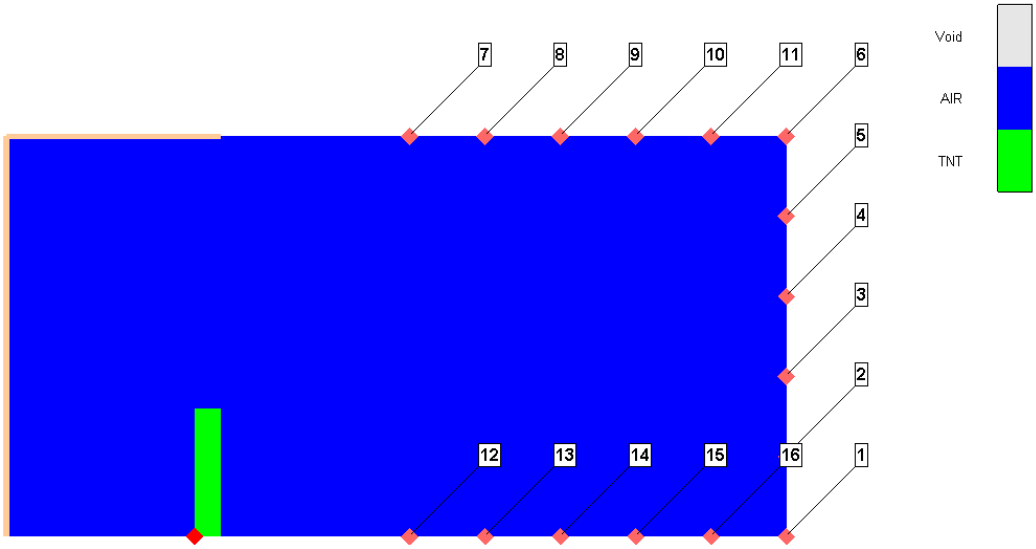

Figure 5: Numerical model for 4g of PE4 and 75 mm of stand-off distance. Axial symmetry. 2D model. Mesh: 105.2 x 53 mm mesh representing a 106 mm-diameter cylinder

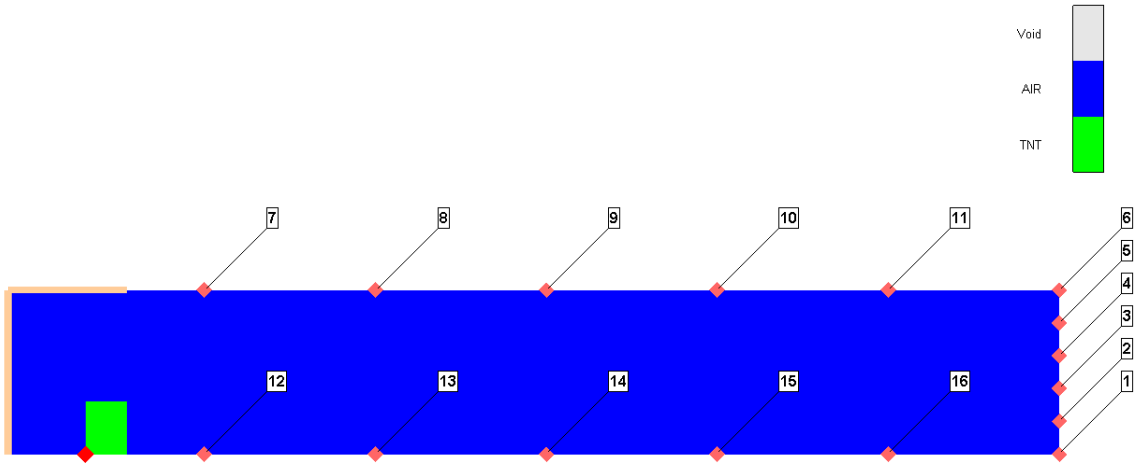

Figure 6: Numerical model for 15g of PE4 and 300 mm of stand-off distance. Axial symmetry. 2D model. Mesh: 344.5 x 53 mm mesh representing a 106 mm-diameter cylinder

3.4 Boundary transmit

In order to fulfil the radiation condition, a transmitting boundary was defined for air as well as soil subgrids external limits. The Transmit Boundary condition allows a stress wave to continue “through” the physical boundary of the subgrid without reflection. The size of the numerical mesh can be reduced by use of this boundary condition. The transmit boundary is only active for flow out of a grid. The transmit boundary is calculated as follows:

Let the normal velocity at the boundary be U_n, where U_n is positive for outflow. Then the

Copyright © 2009 Asociación Argentina de Mecánica Computacional http://www.amcaonline.org.ar

boundary pressure (P) is computed as follows:

For $U_n > 0$:

$$P = P_{ref} + (U_n - U_{ref})I \tag{3}$$

For $U_n < 0$:

$$P = P_{ref} \tag{4}$$

in which P_{ref} and U_{ref} are the pressure and velocity of reference respectively (material model properties) and I is the material impedance (density*soundspeed). If the impedance at the boundary is undefined, it is taken from values in adjacent cells.

Although the boundary transmit was applied to all models, an additional distance of 25 mm of air was included in the back of the explosive to prevent spurious reflections (see Figures 5 and 6).

4 NUMERICAL RESULTS AND DISCUSSION

4.1 Wave propagation

In order to illustrate the wave propagation in tubes of different length, the propagation of the blast wave for the cases: a) 4g of PE4 and 75mm of stand-off distance and b) 15g of PE4 and 200mm of stand-off distance; is presented in Figures 7 and 8.

It can be clearly observed in Figure 8 how the reflection from the wall of the tube (an enhanced shock) interacts with the original shock wave to produce a resultant shock front known as the "Mach front". Moreover, in the case (a) the shock wave arrives first to the central point of the plate and, in the case (b) the shock front seems to be more uniform.

4.2 Overpressures and impulses

The maximum overpressures and impulses over the plate (gauges 1-6) are presented in Tables 2 to 4.

Moreover, the time-history of the overpressures over the plate (gauges 1-6) is shown for some of the cases analyzed in Figures 9 to 12.

Gauge	25mm		50mm		75mm		100mm		200mm		300mm	
	P_r kPa x 10^5	I_r kPa-ms x 10^3	P_r kPa x 10^5	I_r kPa-ms x 10^3	P_r kPa x 10^5	I_r kPa-ms x 10^3	P_r kPa x 10^5	I_r kPa-ms x 10^3	P_r kPa x 10^5	I_r kPa-ms x 10^3	P_r kPa x 10^5	I_r kPa-ms x 10^3
1	5.92	4.84	2.42	2.90	1.53	2.36	1.21	1.58	1.41	1.93	0.50	1.72
2	6.03	3.63	2.13	2.26	0.92	1.98	0.52	1.37	0.65	1.77	0.24	1.57
3	4.46	1.75	1.55	1.50	0.68	1.68	0.49	1.27	0.37	1.59	0.26	1.49
4	1.04	0.70	0.69	1.00	0.48	1.52	0.49	1.21	0.35	1.50	0.26	1.49
5	0.27	0.63	0.28	0.98	0.52	1.51	0.60	1.16	0.35	1.47	0.27	1.53
6	0.57	1.09	0.86	1.25	1.18	1.88	0.78	1.33	0.45	1.49	0.39	1.63

Table 2: Maximum overpressures and impulses for 4g of PE4 and all analyzed distances

Copyright © 2009 Asociación Argentina de Mecánica Computacional http://www.amcaonline.org.ar

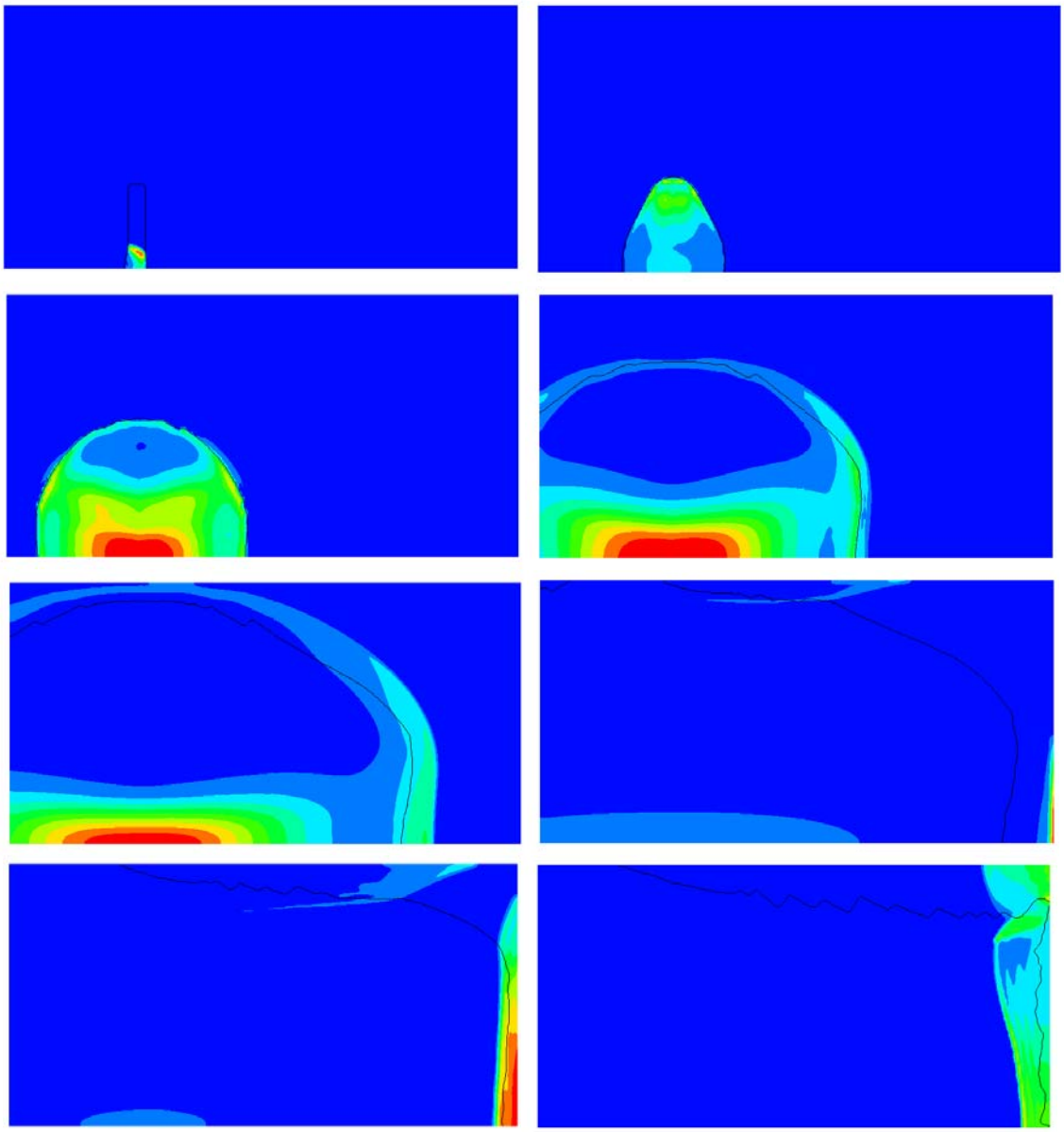

Figure 7: Wave propagation for 4g of PE4 and 75 mm of stand-off distance.

Gauge	25mm		50mm		75mm		100mm		200mm		300mm	
	P_r kPa x 10^5	I_r kPa-ms x 10^3	P_r kPa x 10^5	I_r kPa-ms x 10^3	P_r kPa x 10^5	I_r kPa-ms x 10^3	P_r kPa x 10^5	I_r kPa-ms x 10^3	P_r kPa x 10^5	I_r kPa-ms x 10^3	P_r kPa x 10^5	I_r kPa-ms x 10^3
1	11.9	10.3	3.98	6.33	2.50	5.20	3.70	3.53	3.35	5.33	1.10	3.76
2	12.1	7.65	3.85	4.81	1.40	4.29	0.91	3.02	1.78	4.14	0.43	3.13
3	7.69	3.80	2.59	3.14	1.15	3.57	0.77	2.79	0.80	3.08	0.49	2.88
4	1.43	1.95	1.13	2.10	1.08	3.19	0.12	2.64	0.60	2.47	0.50	2.78
5	0.57	2.00	0.86	2.15	1.19	3.28	0.12	2.49	0.59	2.60	0.56	2.85
6	1.73	3.14	1.62	2.90	1.55	3.90	0.13	2.72	0.60	3.14	0.60	3.15

Table 3: Maximum overpressures and impulses for 9g of PE4 and all analyzed distances

Copyright © 2009 Asociación Argentina de Mecánica Computacional http://www.amcaonline.org.ar

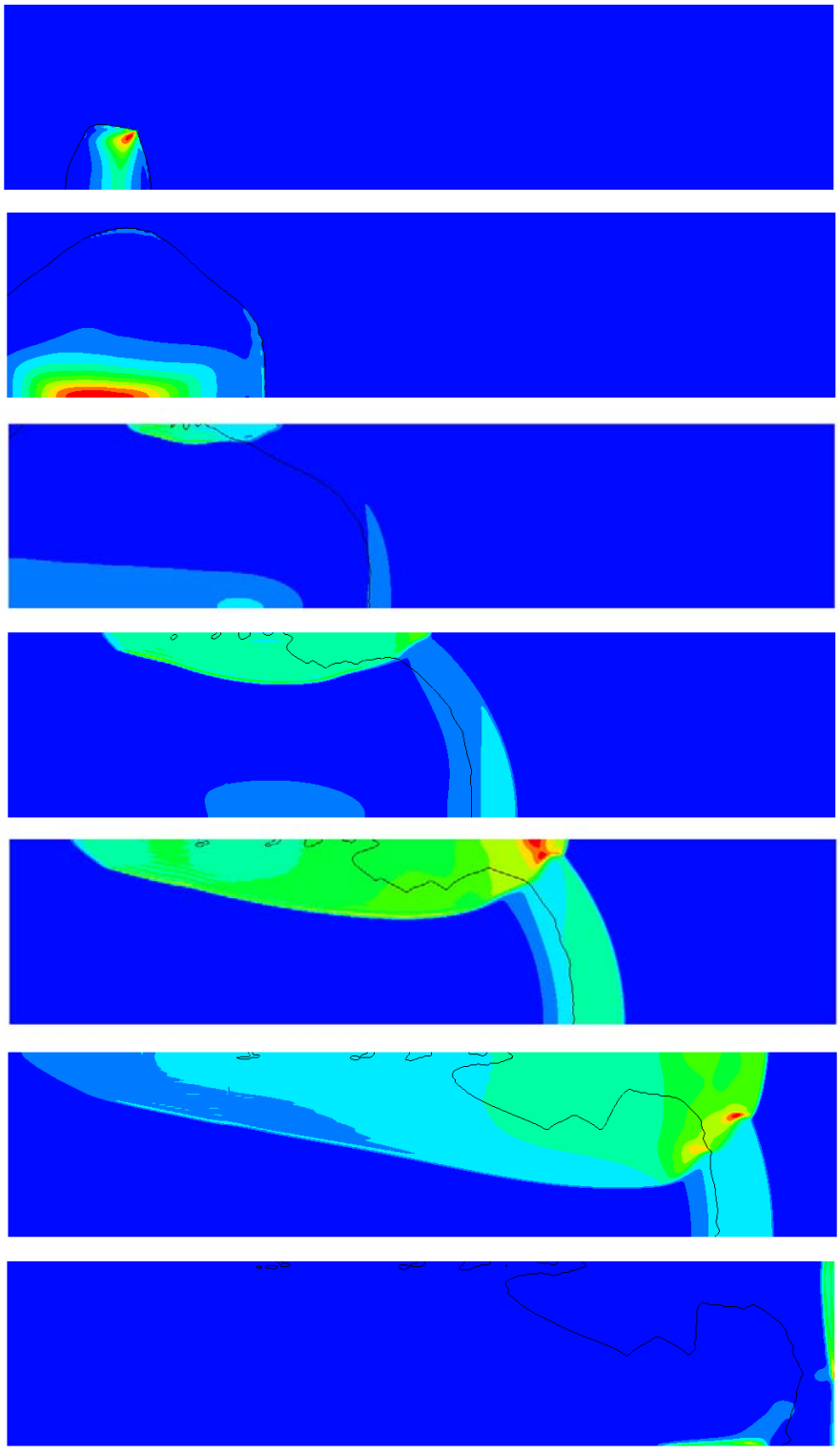

Figure 8: Wave propagation for 15g of PE4 and 200 mm of stand-off distance

Copyright © 2009 Asociación Argentina de Mecánica Computacional http://www.amcaonline.org.ar

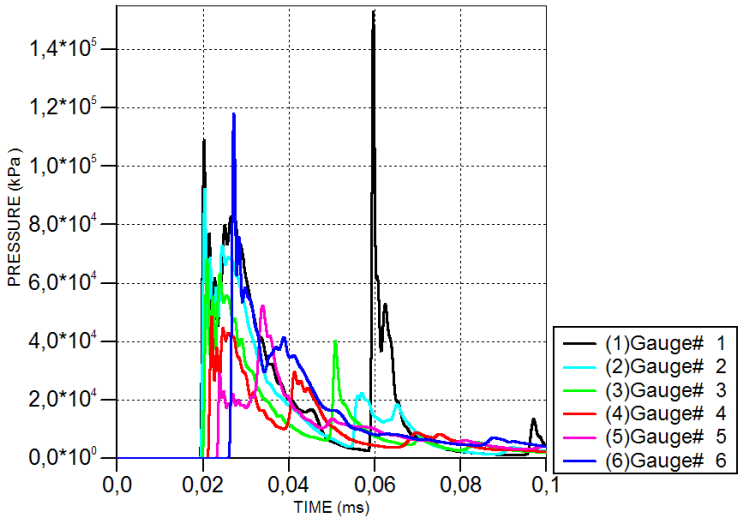

Figure 9: Time-history of overpressures for 4g of PE4 and 75 mm of stand-off distance

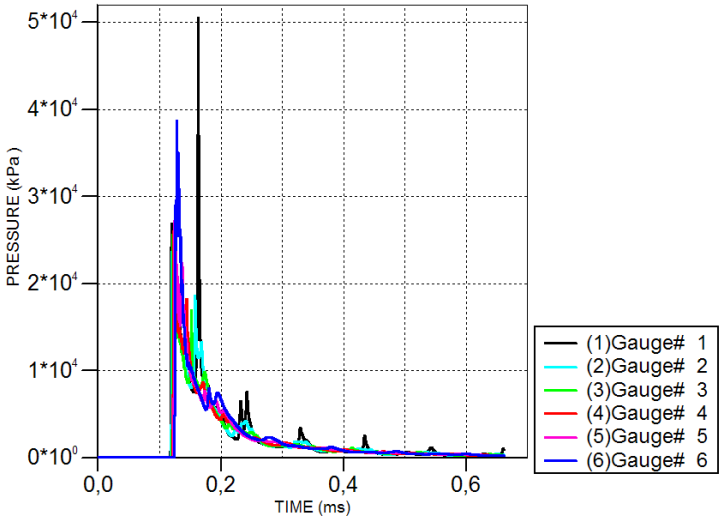

Figure 10: Time-history of overpressures for 4g of PE4 and 300 mm of stand-off distance

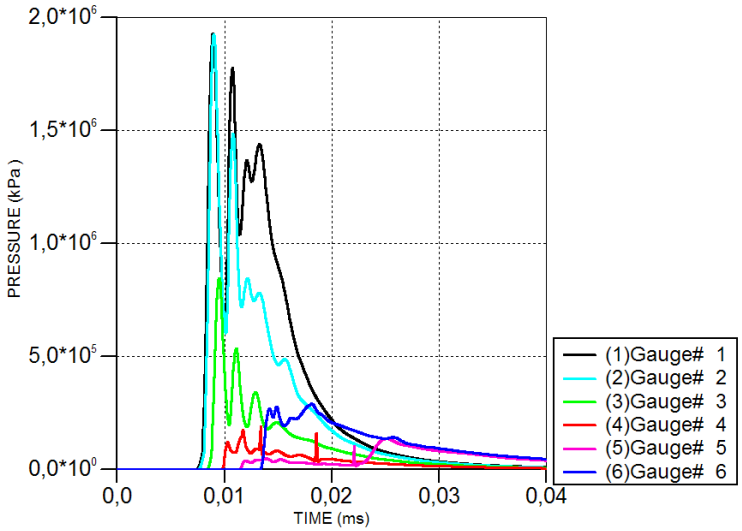

Figure 11: Time-history of overpressures for 15g of PE4 and 25 mm of stand-off distance

Copyright © 2009 Asociación Argentina de Mecánica Computacional http://www.amcaonline.org.ar

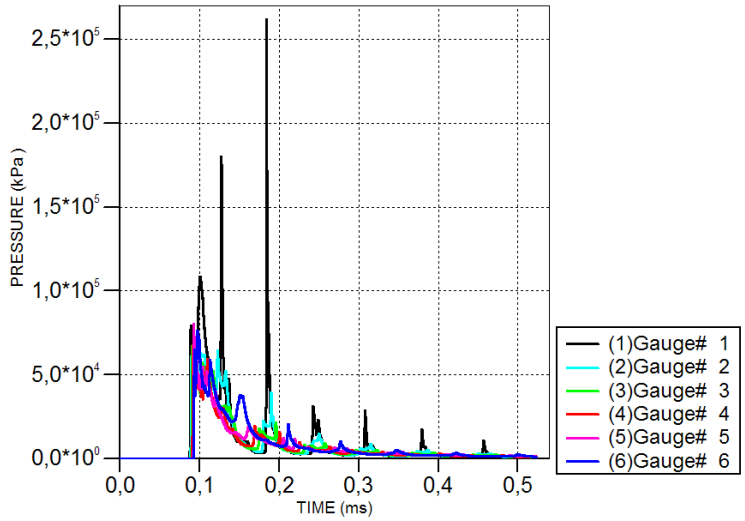

Figure 12: Time-history of overpressures for 15g of PE4 and 300 mm of stand-off distance

Gauge	25mm		50mm		75mm		100mm		200mm		300mm	
	P_r kPa x 10^5	I_r kPa-ms x 10^3	P_r kPa x 10^5	I_r kPa-ms x 10^3	P_r kPa x 10^5	I_r kPa-ms x 10^3	P_r kPa x 10^5	I_r kPa-ms x 10^3	P_r kPa x 10^5	I_r kPa-ms x 10^3	P_r kPa x 10^5	I_r kPa-ms x 10^3
1	19.9	13.8	7.24	9.27	6.81	7.53	6.79	5.47	7.69	9.35	2.61	6.12
2	19.0	10.1	6.35	7.08	2.09	6.01	1.27	4.77	2.65	6.39	0.64	4.88
3	8.80	4.98	5.63	4.71	1.75	5.00	1.10	4.42	1.26	4.75	0.67	4.37
4	2.70	2.67	1.68	3.30	1.70	4.43	1.80	4.24	0.85	3.47	0.67	4.06
5	0.99	2.66	1.81	3.53	2.08	4.59	1.81	3.89	0.77	3.49	0.80	4.15
6	2.75	4.60	2.49	4.62	2.15	5.54	1.65	4.37	0.78	4.72	0.76	4.76

Table 4: Maximum overpressures and impulses for 15g of PE4 and all analyzed distances

In order to compare the results with those obtained by Jacob et al. (2007), in Figures 13 to 16 are presented the variation of the maximum overpressures and impulses versus the stand-off distances for the gauges 1 and 2, near of the center of the plate (see figures 5 and 6). Jacob et al. (2007) shown that the midpoint deflections are similar for stand-off distances ranging from 75 to 300 mm for a given charge mass (Fig. 9 by Jacob et al. 2007). This result is qualitatively confirmed for the results of this paper and presented in Figures 13 to 16 in terms of overpressures and impulses that are the responsible for the permanent deflections of the plates.

4.3 Influence of the confinement

In order to study the influence of the confinement give for the tubes in the propagation of the blast wave, in Tables 5 and 6 a comparison of the maximum overpressures and impulses for some cases with and without tube is presented. It can be seen in Tables 5 and 6 that for small stand-off distances (25 mm) the overpressures and impulses at the center of the plate (gauges 1 and 2) are similar. Moreover, for long stand-off distances (100 and 300 mm) the "mach effect" is very significant, clearly increasing the overpressures and impulses at the center of the plate.

Copyright © 2009 Asociación Argentina de Mecánica Computacional http://www.amcaonline.org.ar

On the other hand, near of the support of the plate (gauges 5 and 6) the effect of increasing overpressures and impulses is similar for small and long stand-off distances.

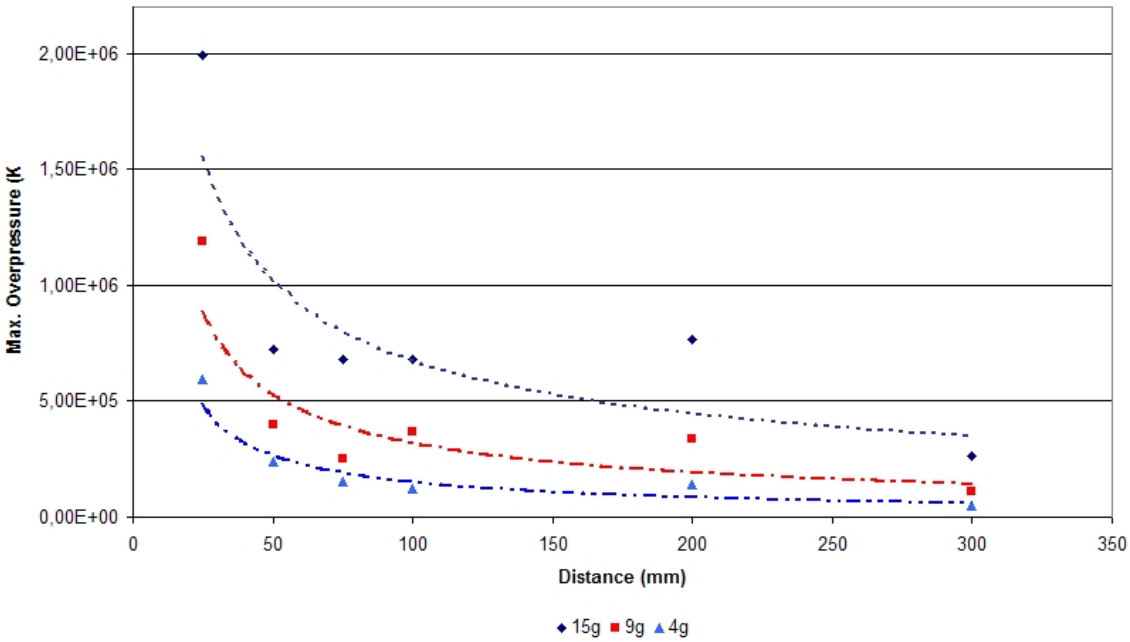

Figure 13: Maximum overpressure versus stand-off distance. Point 1.

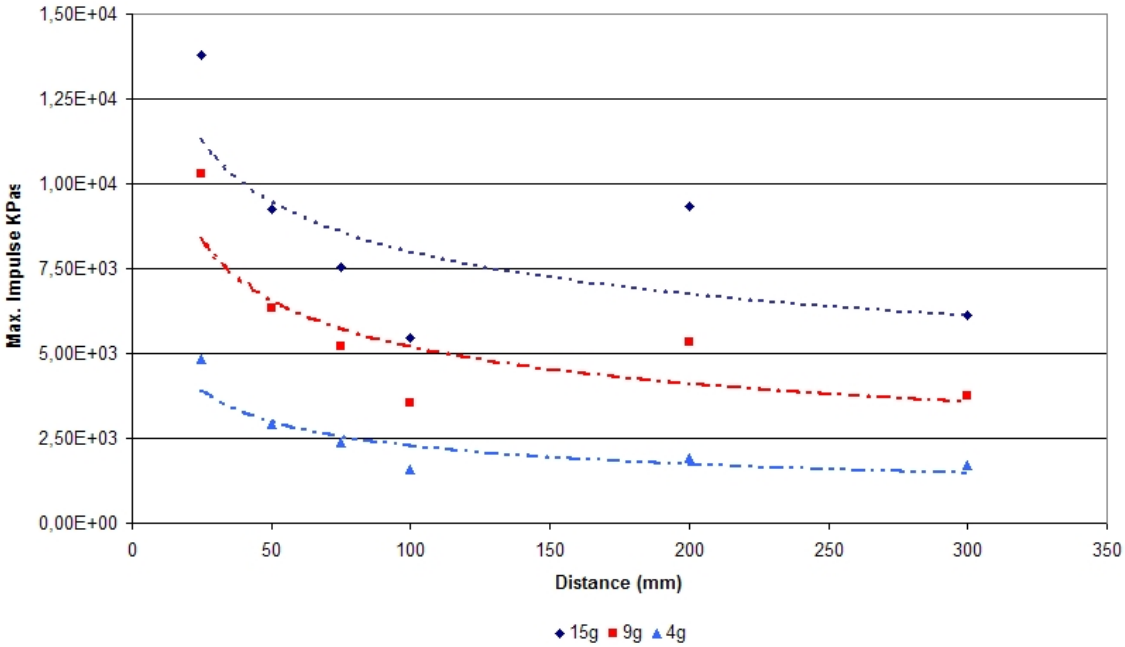

Figure 14: Maximum impulse versus stand-off distance. Point 1.

Copyright © 2009 Asociación Argentina de Mecánica Computacional http://www.amcaonline.org.ar

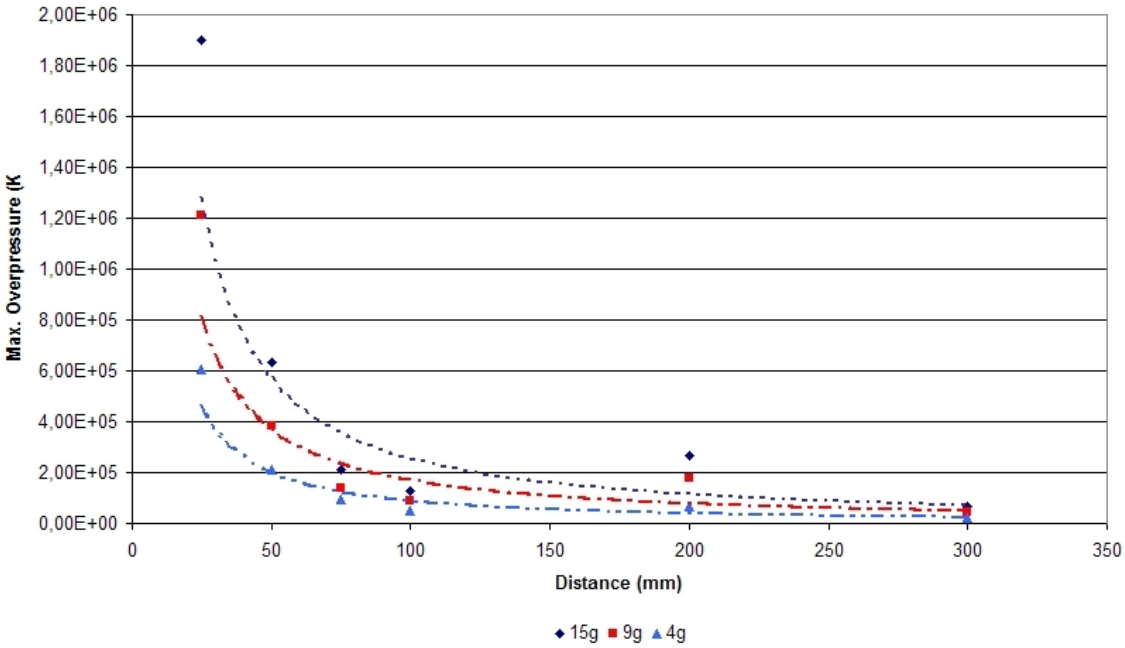

Figure 15: Maximum overpressure versus stand-off distance. Point 2.

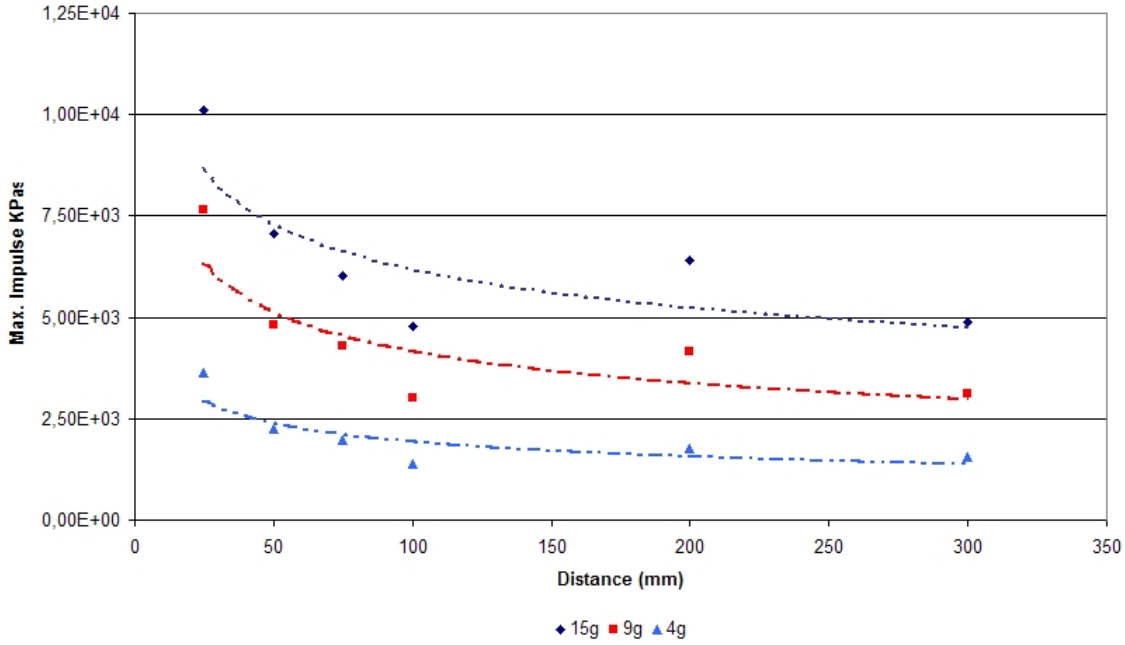

Figure 16: Maximum impulse versus stand-off distance. Point 2.

Copyright © 2009 Asociación Argentina de Mecánica Computacional http://www.amcaonline.org.ar

Gauge	25mm with tube		25mm without tube		Diff		100mm with tube		100mm without tube		Diff.	
	P_r kPa x 10^5	I_r kPa-ms x 10^3	P_r kPa x 10^5	I_r kPa-ms x 10^3	$P_{rt/}$ P_{rwt}	$I_{rt/}$ I_{rwt}	P_r kPa x 10^5	I_r kPa-ms x 10^3	P_r kPa x 10^5	I_r kPa-ms x 10^3	$P_{rt/}$ P_{rwt}	$I_{rt/}$ I_{rwt}
1	5.92	4.84	5.73	4.55	1.03	1.06	1.21	1.58	0.51	0.71	2.36	2.23
2	6.03	3.63	6.05	3.44	1.00	1.06	0.52	1.37	0.51	0.68	1.01	2.02
3	4.46	1.75	4.25	1.57	1.05	1.11	0.49	1.27	0.48	0.60	1.01	2.11
4	1.04	0.70	0.77	0.49	1.34	1.44	0.49	1.21	0.41	0.51	1.18	2.37
5	0.27	0.63	0.26	0.20	1.02	3.19	0.60	1.16	0.31	0.42	1.91	2.75
6	0.57	1.09	0.17	0.10	3.37	10.5	0.78	1.33	0.20	0.28	3.91	4.68

Table 5: Maximum overpressures and impulses for 4g of PE4 with and without tube.

Gauge	25mm with tube		25mm without tube		Diff		300mm with tube		300mm without tube		Diff.	
	P_r kPa x 10^5	I_r kPa-ms x 10^3	P_r kPa x 10^5	I_r kPa-ms x 10^3	$P_{rt/}$ P_{rwt}	$I_{rt/}$ I_{rwt}	P_r kPa x 10^5	I_r kPa-ms x 10^3	P_r kPa x 10^5	I_r kPa-ms x 10^3	$P_{rt/}$ P_{rwt}	$I_{rt/}$ I_{rwt}
1	19.9	13.8	19.3	12.2	1.03	1.13	6.79	5.47	0.15	0.60	17.3	10.2
2	19.0	10.1	19.2	8.90	0.99	1.13	1.27	4.77	0.15	0.60	4.29	8.16
3	8.80	4.98	8.45	3.49	1.04	1.43	1.10	4.42	0.15	0.60	4.58	7.28
4	2.70	2.67	1.76	1.18	1.53	2.26	1.80	4.24	0.14	0.59	4.85	6.93
5	0.99	2.66	0.49	0.53	2.03	4.98	1.81	3.89	0.13	0.57	6.18	7.26
6	2.75	4.60	0.28	0.33	9.89	14.0	1.65	4.37	0.12	0.52	6.44	9.14

Table 6: Maximum overpressures and impulses for 15g of PE4 with and without tube.

4.4 Load distribution

In order to study the distribution of overpressures and impulses with the different stand-off distances cannot be compared straightforwardly the maximum overpressures and impulses as it is illustrated in Figure 17. It is clear in this Figure that, in the case of 9g and 300mm, the distribution of overpressure over the plate is approximately uniform meanwhile the maximum overpressure of the point 1 is produced in other time as consequence of the multiple reflections inside the tube. For this reason, the values of overpressures and impulses that are produced when the first pulse of the blast wave arrives must be compared.

Finally, in Figures 18 and 19 is shown the distribution of overpressures and impulses over the plate for the case of 15g of PE4 and all stand-off distances. It can be seen that considering the overpressures, an uniform distribution only can be considered for 300m of stand-off distance. On the other hand, of the point of view of impulses, an approximately uniform distribution can be adopted since 100mm of stand-off distance.

Copyright © 2009 Asociación Argentina de Mecánica Computacional http://www.amcaonline.org.ar

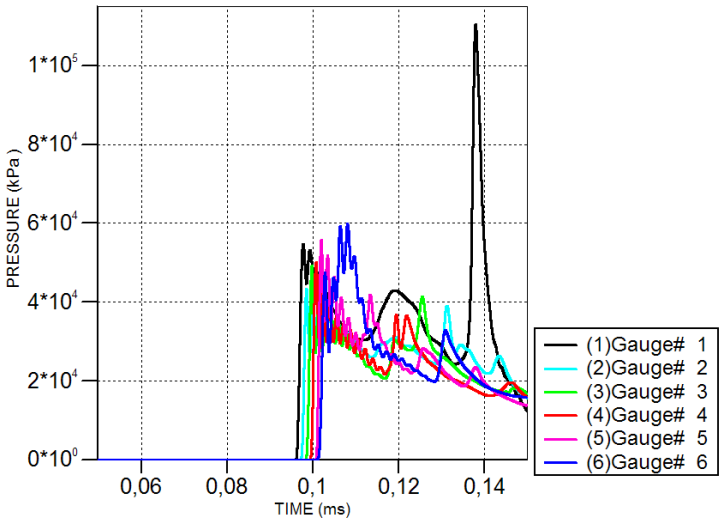

Figure 17: Time-history of overpressures for 9g of PE4 and 300 mm of stand-off distance

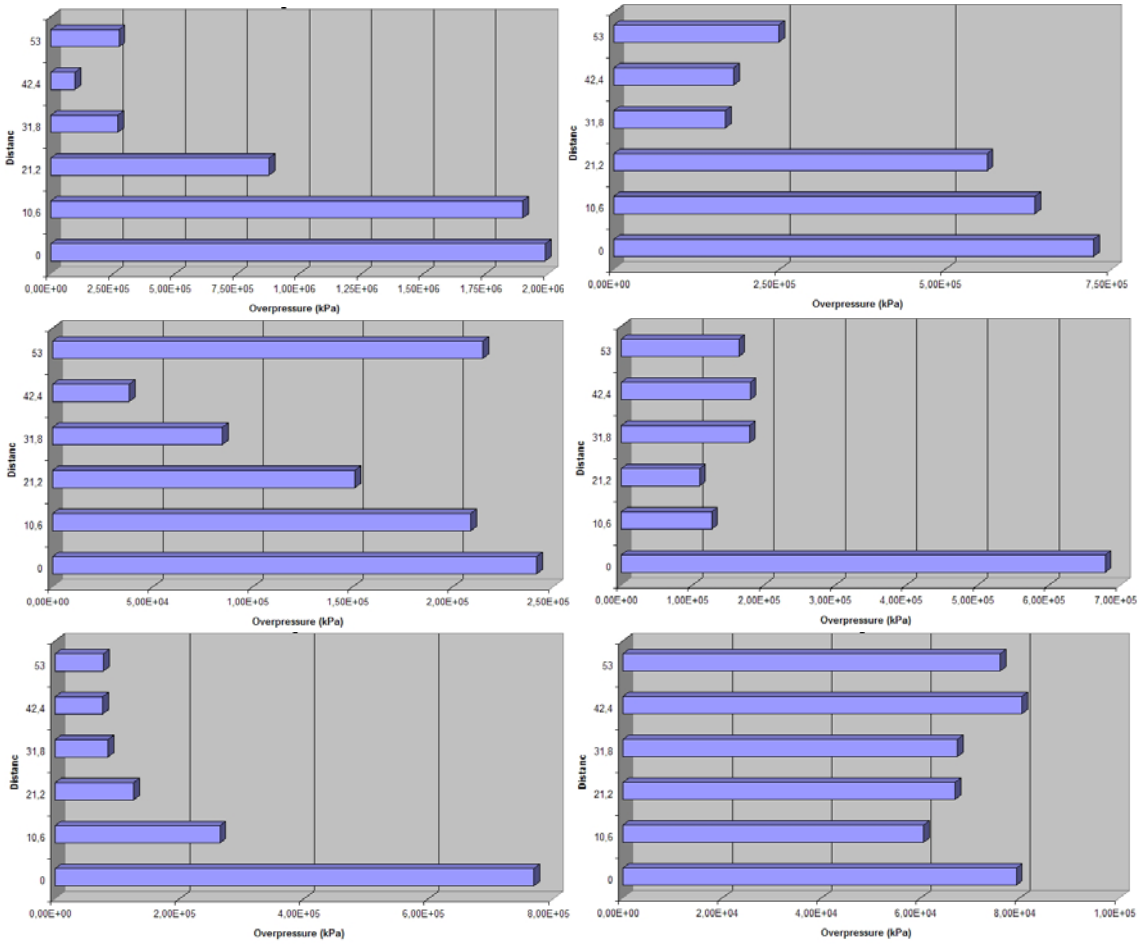

Figure 18: Overpressure distribution for 15g of PE4 and 25, 50, 75, 100, 200 and 300 mm of stand-off distance.

Copyright © 2009 Asociación Argentina de Mecánica Computacional http://www.amcaonline.org.ar

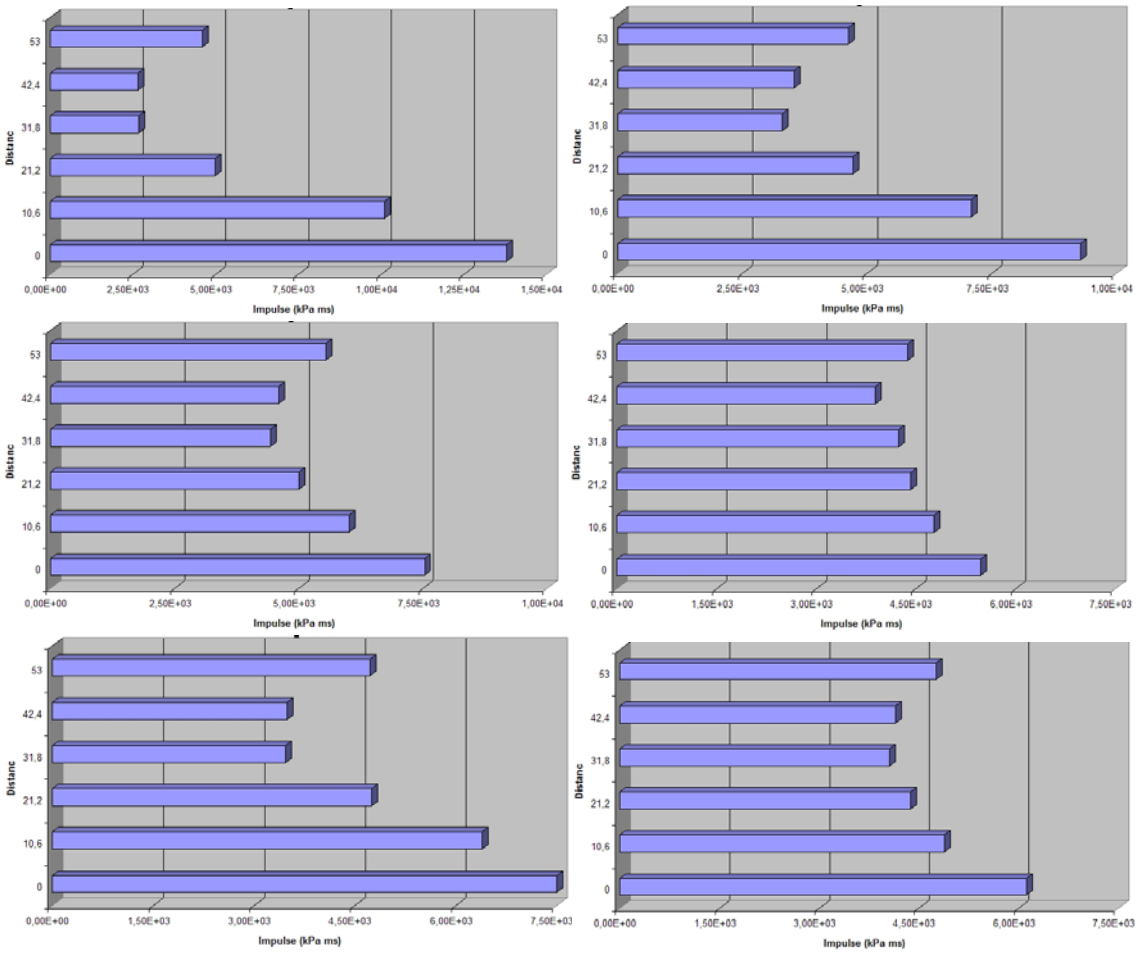

Figure 19: Impulse distribution for 15g of PE4 and 25, 50, 75, 100, 200 and 300 mm of stand-off distance.

5 CONCLUSIONS

A numerical study about the wave propagation in a set of experimental tests on clamped circular mild steel plates, of radius 53 mm, subjected to blast loads travelling along tubular structures that was carried out at the Blast Impact and Survivability Research Unit (BISRU, University of Cape Town). The stand-off distance is varied from 25 to 300 mm, and the load masses are varied from 4 to 15 g.

Based on the obtained results, the following conclusions must be drawn:

- It can be clearly observed in Figure 8 how the reflection from the wall of the tube (an enhanced shock) interacts with the original shock wave to produce a resultant shock front known as the "Mach front", particularly in long tubes.
- Jacob et al. (2007) shown that the midpoint deflections are similar for stand-off distances ranging from 75 to 300 mm for a given charge mass. This result is qualitatively confirmed for the results of this paper mainly in terms of impulses that are the responsible for the permanent deflections of the plates.
- Comparing the results with and without tube, it can be seen that for small stand-off distances the overpressures and impulses at the center of the plate are similar. Moreover, for long stand-off distances the "mach effect" is very significant, clearly

Copyright © 2009 Asociación Argentina de Mecánica Computacional http://www.amcaonline.org.ar

increasing the overpressures and impulses at the center of the plate. On the other hand, near of the support of the plate the effect of increasing overpressures and impulses is similar for small and long stand-off distances.

- It is shown that considering the overpressures, an uniform distribution only can be considered for long stand-off distance. On the other hand, of the point of view of impulses, an approximately uniform distribution can be adopted since medium stand-off distances.

In future papers, the influence of the flexibility of the plate will be studied.

ACKNOWLEDGEMENTS

The financial support of the CONICET (Argentina), SECYT (National University of Cuyo), CIUNT (National University of Tucumán), the National Research Foundation (South Africa) and MINCYT (Argentina) is gratefully acknowledged.

REFERENCES

AUTODYN. *Interactive Non-Linear Dynamic Analysis Software*, Version 11.0, User's Manual. Century Dynamics Inc., 2007

Baker W.E., Cox P.A., Westine P.S., Kulesz J.J., Strehlow R.A., *Explosion hazards and evaluation*. Elsevier, Amsterdam. 1983.

Chung Kim Yuen S, Nurick GN. The significance of the thickness of a plate when subjected to localised blast loads. *Proc 16th int symp military aspects of blast and shock*. 491–499, 2000.

Cowler MS, Hancock SL. Dynamic fluid-structure analysis of shells using the PISCES 2DELK computer code. *5th Int. Conf. on Structural Dynamics in Reactor Technology,* Paper B1/6, 1979.

Hancock S. Finite Difference Equations for PISCES-2DELK, TCAM-76-2, *Physics International*, 1976.

Jacob N, Chung Kim Yuen S, Bonorchis D, Nurick GN, Desai SA, Tait D. Quadrangular plates subjected to localised blast loads — An insight into scaling. *International Journal of Impact Engineering,* 30(8–9): 1179–1208, 2004.

Jacob N., Nurick GN, Langdon GS. The effect of stand-off distance on the failure of fully clamped circular mild steel plates subjected to blast loads. *Engineering Structures,* 29, 2723–2736, 2007.

Kinney G.F., Graham K.J. *Explosive shocks in air*. 2nd Edition, Springer Verlag, 1985.

Lee, E. L., & Tarver, C. M.. Phenomenological Model of Shock Initiation in Heterogeneous Explosives. *Physics of Fluids*, 23 (12), 2362-2372 1980.

Nurick GN, Martin JB. Deformations of thin plates subjected to impulsive loading — A review; Part I — Theoretical consideration. *International Journal of Impact Engineering* 8(2), 159–70, 1989.

Nurick GN, Radford AM. Deformation and tearing of clamped circular plates subjected to localised central blast loads. *Recent developments in computational and applied mechanics: A volume in honour of John B. Martin. Barcelona (Spain)*: International centre for numerical methods in engineering (CIMNE); p. 276–301, 1997.

Schleyer GK, Hsu SS, White MD, Birch RS. Pulse pressure loading of clamped mild steel plates. *International Journal of Impact Engineering*, 28, 223–47, 2003.

Smith PD, Hetherington JG, *Blast and Ballistic Loading of Structures*, Butterworth-Heinemann Ltd, Great Britain. 1994.

Teeling-Smith RG, Nurick GN. The deformation and tearing of circular plates subjected to

Copyright © 2009 Asociación Argentina de Mecánica Computacional http://www.amcaonline.org.ar

impulsive loads. *International Journal of Impact Engineering*, 11(1), 77–92, 1991.
Wharton RK, Formby SA, Merrifield R. Air-blast TNT equivalence for a range of commercial blasting explosives. *Journal of Hazardous Materials,* A79, 31–39, 2000.
Wilkins, M. L. Calculation of Elastic-Plastic Flow, *Methods of Computational Physics*, 3, 211-263 1964.
Yang R, Bawden WF, Katsabanis PD. A New Constitutive Model for Blast Damage, *Int. J. Rock Mech. Min. Sci. & Geomech*. Abstr., 33(3), 245-254. 1996.
Youngs, DL. Time-Dependent Multimaterial Flow with Large Fluid Distortion, *Numerical Methods for Fluid Dynamics*, 1982.

Copyright © 2009 Asociación Argentina de Mecánica Computacional http://www.amcaonline.org.ar